RESEARCH PAPER

Castor Folate Ester Niosomes: Enhancing Doxorubicin Hydrochloride Delivery and Stability

Amin Rahiminejad, Mojgan Heydari*, Fariba Tajabadi

* *M.Heydari@merc.ac.ir*

Department of Nano Technology and Advanced Materials, Materials and Energy Research Center, Karaj, Iran

Received: February 2025 **Revised: March 2025** **Accepted: March 2025**
DOI: 10.22068/ijmse.3913

Abstract: *Targeted drug delivery systems have been developed to overcome the disadvantages of conventional drug delivery systems, and folate is one of the targeting molecules that has received attention in recent years. The attachment of this molecule to the surface of niosomal carriers has been achieved using Castor oil as an intermediate molecule. We incorporated CF into a noisome structure as a biocompatible component for targeted delivery of the anticancer drug Doxorubicin. This research studies the novelty of castor folate ester in the scope of niosome-based drug delivery systems. The aim was to investigate the feasibility of manufacturing and evaluating a niosomal carrier containing the drug DOX and its targeting by the combination of CF. The results of FTIR confirm chemical bonding between folic acid and castor oil. SEM showed good morphology with spherical structure of niosomes. These niosomes have particle sizes of 330 to 538 nm for different samples. Also, the zeta potential was -28 to -40 mV, which resulted in good stability. Adding CF to niosomal samples increased wettability and drug loading efficacy, and potential results from DLS and zeta confirm the folate impact on surface hydrophilicity of niosome spheres. The prepared formulations increased the effectiveness of doxorubicin on L929 fibroblast cells. The proposed biocompatible component showed the role of CF in the architectural integrity of niosomal lipid bilayers.*

Keywords: *Castor folate ester, Niosome formulation, Doxorubicin hydrochloride, Colloidal stability, Drug delivery.*

1. INTRODUCTION

The emergence of targeted drug delivery systems (DDS) signifies a substantial advancement in contemporary therapeutic technologies [1]. Niosomes, vesicles composed of non-ionic surfactants, have proven to be an up-and-coming option within this field. Their biocompatibility and stability are unmatched, and they inherently can encapsulate a broad spectrum of drugs [2, 3]. Surface-modifying these systems is a suitable method to deliver therapeutic agents to precise locations within the body, optimizing efficacy and reducing potential adverse effects [4].

The concept of niosomes as a drug delivery vehicle has been thoroughly investigated in the literature, with numerous studies emphasizing their potential to enhance the bioavailability and therapeutic efficacy of a range of drugs. Niosomes are recognized for their capacity to encapsulate hydrophilic and lipophilic drugs, safeguard them from degradation, and facilitate controlled release at the target site [2, 3, 5, 6]. A review by Paliwal et al. offers an exhaustive overview of niosome formulations, outlining their benefits, such as biodegradability, non-immunogenicity, and versatility in administration routes [7]. Furthermore, the work of Moghtaderi et al. examines the structural components of niosomes, exploring the role of surfactants and cholesterol in vesicle formation and stability, which are essential elements in the creation of an effective niosome-based drug delivery system [8]. Nanoscale vesicular systems have the passive targeting ability. This means they can accumulate in targeted cancer tissues and release the drug before it is taken into the target cell by endocytosis. On the other hand, actively targeting tumor cells by modifying the surface of nanoparticles can significantly enhance their internalization. This mechanism targets receptors on the surface of cancer cells and delivers drugs into the cells [9]. Folic acid has been extensively researched as a drug-delivery targeting agent due to its high affinity for the folate receptor, which is overexpressed in several cancer types. The literature presents numerous nanoparticle systems modified with folic acid to achieve targeted delivery. For example, research by Wang et al, illustrated the successful targeting and treatment of cancer cells using folic acid-conjugated nanoparticles, leading to improved cellular uptake and therapeutic results [10]. Similarly, a study by Bahrami et al. examined folic acid-modified liposomes for delivering anticancer drugs, yielding promising outcomes regarding specificity and

[DOI: 10.22068/ijmse.3913]

diminished toxicity [11]. In another Safari Sharafshadeh et al. study, folic acid in the form of DSPE-PEG (2000)-folate was used to decorate niosomes and target breast and ovarian cancer cell lines. This study demonstrated the ability to simultaneously combine treatments and target cancer cell lines [12]. These studies highlight the potential of folic acid as a targeting agent.

In recent years, studies have been conducted on using PEG-folate combinations in vesicular systems to target cancer cells, and the results indicated increased drug targeting and reduced side effects. PEGylation has benefits in niosomal vesicles, some of which include increased circulation time in the bloodstream and preventing opsonization [13, 14]. Some research has also focused on the disadvantages of using PEG in drug delivery systems, citing the synthetic nature of this material as a reason for its toxicity to body cells [15]. To synthesize targeted niosomal carriers, we need to use natural functional groups that are non-toxic and castor oil is one of them.

Castor oil is characterized by its unique hydroxyl functional group, making it an ideal candidate for chemical modification and subsequent application in drug delivery systems [16]. The conjugation of castor oil with folic acid has resulted in the creation of castor folate, a compound that combines the lipophilic properties of castor oil with the targeting capabilities of folic acid [17]. This synthesis was postulated to significantly enhance the delivery of doxorubicin hydrochloride, a potent chemotherapeutic agent, directly to cancer cells, thereby improving treatment outcomes. Castor folate is integrated into the niosome's bilayer structure to enhance the targeted delivery of doxorubicin hydrochloride. Although folic acid and its derivatives have been thoroughly studied as targeting ligands in various nanoparticle systems [11, 12], their integration into niosome bilayers in castor folate is an innovative concept that has not been previously explored. This study seeks to bridge this gap by synthesizing castor folate and evaluating its role in enhancing the targeting efficiency of niosomes towards cancer cells.

This is the first instance of castor oil being esterified with folic acid to create castor folate, which is then employed as a key component of the niosome bilayer. This innovation is expected to utilize the folate receptor-mediated endocytosis pathway, which is overexpressed in various cancer cell types [18, 19].

2. EXPERIMENTAL PROCEDURES

2.1. Materials

Folic acid and castor oil, procured from Sigma-Aldrich, served as the foundational components for the novel castor folate compound, with the former acting as a targeting moiety and the latter providing a lipophilic base. The synthesis was performed by N,N-Dimethylformamide (DMF) and Triethylamine, sourced from Merck, which acted as the solvent and base. The coupling reaction was driven by 2-(1H-Benzotriazole-1-yl)-1,1,3,3-tetramethylaminium Tetrafluoroborate (TBTU), obtained from Sigma-Aldrich, while post-reaction purification involved Dichloromethane (DCM), Sodium Bicarbonate (NaHCO□), and Sodium Sulfate (Na□SO□), all from Merck, to ensure the removal of byproducts and excess reagents.

The niosome formulation was synthesized using Cholesterol and Sorbitan Monostearate (Span 60) from Sigma-Aldrich, which provided structural integrity and stability to the vesicles, and Dicetyl Phosphate from Merck, which imparted the necessary surface charge. The vesicles were buffered in Phosphate-Buffered Saline (PBS) from Merck, creating an isotonic environment for the encapsulation of Doxorubicin Hydrochloride, the chemotherapeutic agent chosen for its efficacy in cancer treatment, sourced from Sigma-Aldrich. Each material was utilized without further modification, relying on their analytical grade to ensure consistency and reproducibility in the experimental outcomes.

2.2. Castor-Folate (CF) Synthesis

In an initial reaction step, 0.441 g (1 mmol) of folic acid was transferred into a 25 ml round-bottom flask and solubilized in 5 mL of anhydrous DMF. The reaction sequence added 0.706 g (2.2 mmol) of TBTU and 0.405 g (4 mmol) of triethylamine. The mixture underwent magnetic stirring for 30 minutes at 25°C. Subsequently, 0.280 g (0.3 mmol) of castor oil was introduced to the reaction vessel. The system was maintained under agitation for 5 hours at 25°C. Post-reaction, the product extraction entailed the addition of 15 ml of DCM, followed by sequential washes with distilled H_2O, 5% HCl, saturated $NaHCO_3$ solution, and anhydrous

[DOI: 10.22068/ijmse.3913]

Na_2SO_4. The organic phase was then subjected to solvent evaporation under reduced pressure in a vacuum oven, culminating in isolating the target compound, castor folate (CF) [20]. The successful synthesis of the CF was confirmed via Fourier-transform infrared spectroscopy (FTIR), ensuring the integrity of the molecular structure.

2.3. Niosome Preparation

A lipid mixture comprising cholesterol, Span 60, and dicetyl phosphate was dissolved in 10 mL of chloroform within a 50-mL conical centrifuge tube to synthesise the base formulation. The molar ratio of cholesterol to Span 60 to dicetyl phosphate was maintained at 47.5:47.5:5 across all formulations. The chloroform was subsequently removed via rotary evaporation at 160 rpm and 80°C for 30 minutes, yielding a uniform lipid film on the rotary's inner surface. This film was hydrated with 10 mL of a PBS at pH 7.2, containing the chemotherapeutic agent doxorubicin hydrochloride, with a consistent doxorubicin to lipid mass ratio of 0.05. The mixture was agitated vigorously. Niosome formation was induced by sonicating the suspension for 5 min in an ice bath using a sonicator. The CODYSON Digital Ultrasonic Cleaner, CD-4820, was made in China. It was performed with a power of 170 watts and a frequency of 35 kHz. In Niosomes containing CF, differential mass fractions of the conjugate were integrated into the lipid phase before hydration. The formulation devoid of castor-folate was designated as B, while those containing 5, 10, and 15 wt.% of CF were termed CF1, CF2, and CF3, respectively [21, 22].

2.4. Characterization

2.4.1. Fourier-transform infrared (FTIR) spectroscopy

Fourier-transform infrared (FTIR) spectroscopy was carried out to analyze the chemical reaction between folic acid and castor oil, utilizing an EQUINOX 55 (BRUKER) spectrometer made in Germany.

2.4.2. Scanning electron microscopy (SEM)

Scanning Electron Microscopy (SEM) is critical for confirming the vesicular structure and size distribution of the niosomes, which are essential parameters for their potential application in targeted drug delivery systems. Vega (Tescan) SEM, which was made in America, carried it out.

2.4.3. Dynamic light scattering (DLS)

This study measured niosomes' mean size and distribution using the dynamic light scattering (DLS) method by Zetasizer Nano ZS, Malvern Instruments Ltd, made in UK.

2.4.4. Zeta potential

The zeta potential of the synthesized niosomes was measured in a phosphate buffer solution with a pH of 7.2 by a zeta potential Brookhaven instrument device, made in the USA.

2.4.5. Water contact angle

The water contact angle measurements of niosome formulations were determined using a KSV-CAM 101 goniometer, made in Finland, a sophisticated instrument for analyzing the shape of liquid droplets on solid substrates. A Hamilton syringe dispensed 20 µL droplets of the formulations onto glass slides, emulating a controlled laboratory environment. The droplet shapes were digitally captured and analyzed with the CAM 101 software, integral to the KSV-CAM 101 system. To ensure the robustness of the experimental data, each measurement was replicated three times. The empirical results obtained from these niosome formulations were rigorously compared to a benchmark control—a DOX solution (0.2 mg/ml in phosphate-buffered saline)—to validate the experimental outcomes [23].

2.4.6. UV-Vis spectroscopy

The ultraviolet–visible spectroscopy (UV–Vis) method was employed to quantify the drug loading and release kinetics from the delivery system by Perkin Elmer, model Lambda 25, made in the USA.

2.4.7. Encapsulation efficiency

The samples were encased in a dialysis bag and submerged in 100 ml of distilled water. This step was performed three times using fresh distilled water each time to maximize the removal of non-encapsulated drugs. Following this, the spectrophotometer was used to measure the absorbance at the drug's maximum wavelength, which for DOX is 498 nm. The concentration of the drug remaining in the solution was calculated based on the standard absorption-concentration ratio. The drug retention rate within the niosomes was then computed using eq. 1.

$$EE(\%) = \frac{W_T - W_F}{W_T} \times 100 \quad (1)$$

Here, EE represents the encapsulation efficiency

[DOI: 10.22068/ijmse.3913]

percentage, W_T is the total concentration of the drug initially loaded into the niosomes, and W_F is the concentration not retained within the niosomes [12].

2.4.8. In vitro release

A dialysis bag method was employed to evaluate the drug's release kinetics from niosomes. Specifically, 2 ml of the drug-laden niosomes were sealed in a dialysis bag and immersed in 100 ml phosphate buffer (pH 7.2) at a controlled temperature of 25°C. The quantity of drug diffusing into the buffer was monitored at pre-determined intervals: 1.5, 3, 4.5, 6, 9, 12, 18, and 24 hours. The release profile was determined by measuring the absorbance of DOX in the buffer and comparing it to a standard solution,

2.4.9. Cytotoxicity

The cytotoxicity of the drug-loaded niosomes was assessed utilizing the MTT assay, a colorimetric method for evaluating cytotoxic levels, in strict adherence to the ISO 10993-5 standards.

The niosomes underwent a thorough toxicity analysis using L929 fibroblast cells. Initially, the niosomes were allocated into 24-well plates, succeeded by seeding L929 cells at a density of (5×10^4) cells/cm² within an RPMI/1640 culture medium, enriched with 10% fetal bovine serum. Subsequently, the samples were incubated at 37°C in an atmosphere containing 5% CO_2 for 24 hours. Following incubation, a specified volume of MTT solution, with a concentration of 1 mg/ml, was dispensed into each well. The culture plates were then placed back into the incubator, protected from light exposure, for a duration ranging between 1 to 3 hours. After this interval, the cells were gently washed with phosphate-buffered saline to remove any unmetabolized MTT. The resultant formazan crystals were dissolved using isopropanol, and the absorbance for each well was accurately measured at a wavelength of 540 nm utilizing an ELISA reader (ELX 808 BioTek, USA). The viability of the cells was determined by comparing the absorbance ratios of the test samples against the control, which utilized a polystyrene container, thus providing an index of cell survival [24].

3. RESULTS AND DISCUSSION

3.1. Castor Folate Synthesis

As depicted in Figure 1, TBTU catalyzed this esterification reaction [25]. Castor oil is characterized by three hydroxyl groups, each with the potential to react with two carboxylic acid groups from folic acid, which results in ester formation [17]. While these hydroxyl groups are structurally identical and of the secondary type, the carboxylic acid groups of folic acid display varying reactivity due to steric hindrance, leading to preferential reaction with TBTU for one of these groups. This selective reactivity highlights the spatial considerations essential in designing lipid-based carriers for hydrophilic substances like folic acid.

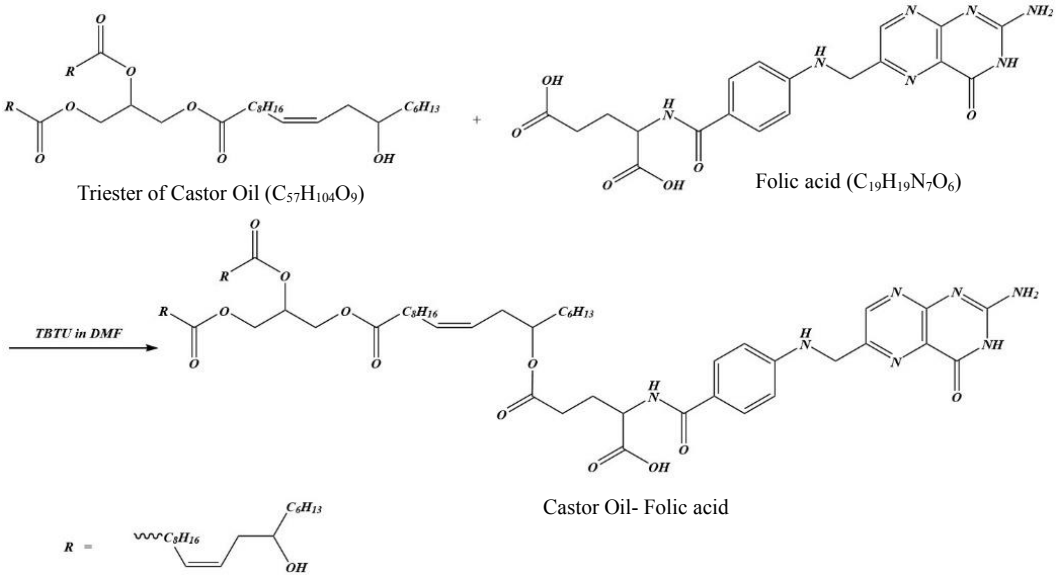

Fig. 1. Schematic of the possible reaction between castor oil and folic acid in the presence of TBTU

[DOI: 10.22068/ijmse.3913]

Figure 1 further illustrates that castor oil's three hydroxy groups can react with folic acid's carboxylic acid groups. The uniformity of the hydroxy groups contrasts with the differential reactivity of the carboxylic acid groups, which is influenced by steric hindrance, resulting in one group being more reactive towards TBTU. This variance in reactivity is a critical factor in the synthesis of lipid-based conjugates intended for biomedical applications.

Figure 2 presents the FTIR spectra of castor oil, folic acid, and the resultant castor-folate product. As determined, the band at 3570 cm^{-1} represents the O-H stretching vibrations in castor oil, which indicate the presence of hydroxylated ricinolic acid. The 2870-2947 cm^{-1} wave numbers correspond to castor oil's aliphatic C-H stretching vibrations. The ester carbonyl (C=O) functional group shows a characteristic stretching band of triglyceride at 1746 cm^{-1}. Also, distinct peaks at 3,340–3,505 cm^{-1} range, related to –NH, –OH bonds in FA, peaks at 3158, 3012 and 2666 cm^{-1} associated with O-H stretching carboxylic acid and strong peak 1706 cm^{-1} observed for carboxylic acid groups.

Notably, the broad peak associated with the carboxylic acid group in folic acid, covering the wavenumbers of 3158, 3012 and 2666 cm^{-1}, is absent in the castor-folate spectrum. Furthermore, the carbonyl group peak in folic acid, initially at 1706 cm^{-1} and marked by a yellow band, shifts to a higher wavenumber (1766 cm^{-1}) in the castor-folate sample. This shift signifies the formation of an ester bond, as ester carbonyl groups absorb at higher wavenumbers than carboxylic acid carbonyls. Additionally, the wavenumbers ranging from 2800-3000 cm^{-1} correspond to the aliphatic C-H stretching vibrations in castor oil, evident in the castor-folate product spectrum. This retention of characteristic peaks confirms the structural presence of castor oil's aliphatic chains in the conjugate, affirming the integrity of the castor oil post-synthesis. The spectral data collectively validate the successful esterification of castor oil and folic acid [26, 27].

3.2. Niosome Characterization

3.2.1. Niosomes' morphology

Niosome surface morphology and size are investigated by SEM analysis. Figure 3 presents the SEM image of the CF1 sample at two magnifications and the CF2 and CF3 niosome samples.

SEM images (sample CF1) were analyzed by Image J software, and the results are shown in Table 1. Further quantitative examination through images reveals that the niosome spheres possess an average particle diameter of approximately 345 nm which is confirmed by the data obtained from the DLS analysis (Table 2). Also, the roundness of the particles is equal to 0.88, indicating preservation of the vesicles' spherical structure in an aqueous environment.

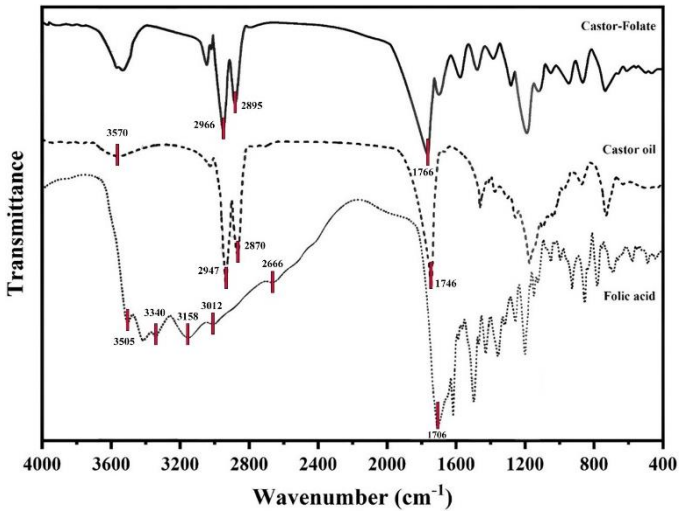

Fig. 2. FTIR spectra of castor oil, folic acid and castor-folate

Table 1. Data obtained from SEM image processing sample CF1 by Image J software

Diameter (nm)	Roundness	Circumference (nm)	Area (nm^2)
345.52 ± 95.50	0.88 ± 0.03	810 ± 224	49266 ± 25.55

[DOI: 10.22068/ijmse.3913]

Table 2. Characteristic features of particle size distribution curves and Zeta potential of samples. Data are mean values ± S.D. (n= 3)

Sample Code	Number Average Particle Size (SN) (d. nm)	Weight Average Particle Size (SW) (d. nm)	Polydispersity Index	Zeta Potential (mv)
B	317.8 ± 19.2	330.2 ± 19.5	0.53 ± 0.02	-28 ± 0.14
CF1	399.2 ± 44.0	415.6 ±46.9	0.56 ± 0.02	-33 ± 0.72
CF2	478.8 ± 23.8	497.4 ± 24.6	0.55 ± 0.01	-36 ± 0.46
CF3	519.0 ± 26.2	537.8 ± 28.8	0.52 ± 0.03	-40 ± 0.17

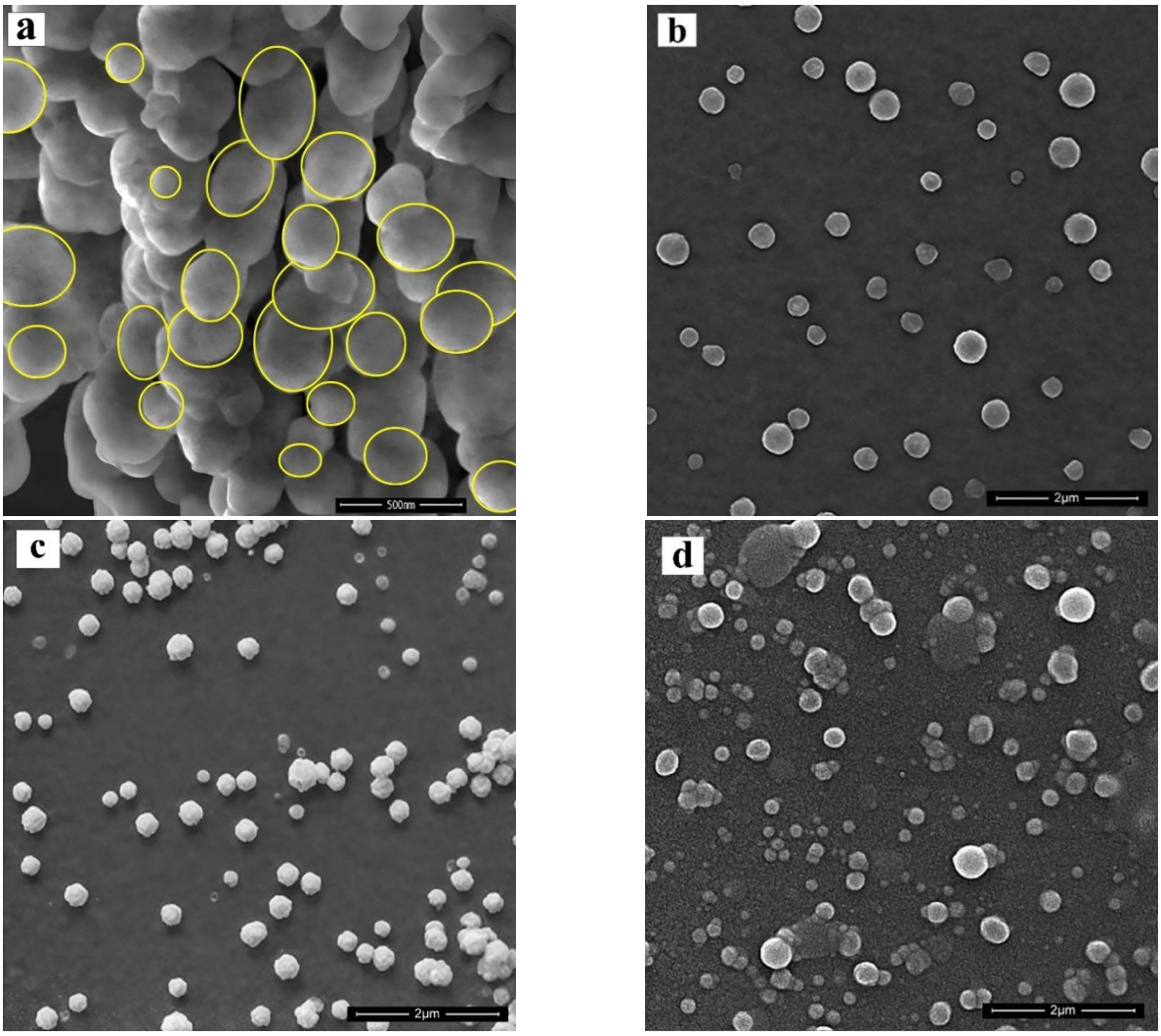

Fig. 3. Scanning electron microscope images of sample CF1 at two magnifications (a) x50 and (b) x200. Sample CF2 (c) and CF3 (d)

3.2.2. Size distribution of niosomes

Figure 3 displays the DLS curve, which represents the size distribution of niosomes, alongside the cumulative particle size curves for various niosome formulations. As can be seen, both the number average and weight average particle size of the niosomal carriers increased with the amount of castor folate in the niosomal samples.

The results of the DLS and zeta potential tests are summarized in Table 2. Sample B has the smallest size with an average of 330 nm, and sample CF3 has the largest size with an average of 538 nm. Increasing the amount of folate in niosomal samples resulted in an increase in particle size due to the hydrophilic nature of the folate molecules [12].

The enhancement in particle size with increasing castor-folate content may be attributed to a rise

[DOI: 10.22068/ijmse.3913]

in the hydrophilic-lipophilic balance (HLB) of the niosome's lipid wall [21]. The folate moiety, known for its substantial hydrophilic properties, enhances the hydrophilicity of the niosome wall when integrated into niosomes. This results in increased water uptake and an enlarged particle size. Despite these changes, the PDI, which indicates the size distribution of niosomal particles in the samples, varies between 0.52 to 0.56 and remains relatively consistent across all niosome formulations, indicating that the variation in the lipid wall composition does not significantly alter the uniformity of the particle sizes. Zeta potential indicates the level of surface charge, and increasing it results in greater stability of niosomal vesicles during storage and administration. Caster–folate–free noisome (sample B) demonstrates a zeta potential of -28 mV, which increases to -33 with the addition of castor folate (sample CF1) and also to -40 in sample CF3, which has the highest amount of castor folate. An observed trend is that with an increased concentration of castor-folate, the zeta potential shifts to more negative values. This shift indicates a rise in the hydrophilic and polar folate groups on the niosome surface, which can be attributed to the successful incorporation of folic acid into the niosome structure, potentially increasing the niosome's stability [12].

3.2.3. Water contact angle of niosomes

The water contact angle (θ), a definitive measure of a liquid's propensity to spread across a solid interface, is critically influenced by the molecular composition of the interacting surfaces [23]. The molecular architecture of the niosomes, wherein lipophilic constituents such as cholesterol are sequestered within the vesicular bilayer, while hydrophilic compounds—most notably, the folic acid present in castor folate ester—are oriented outwardly, accentuates the amphiphilic character of the formulation. This orientation ensures that the hydrophilic entities are preferentially positioned to engage with the aqueous environment, thereby augmenting the niosomes' affinity for hydrophilic surfaces.

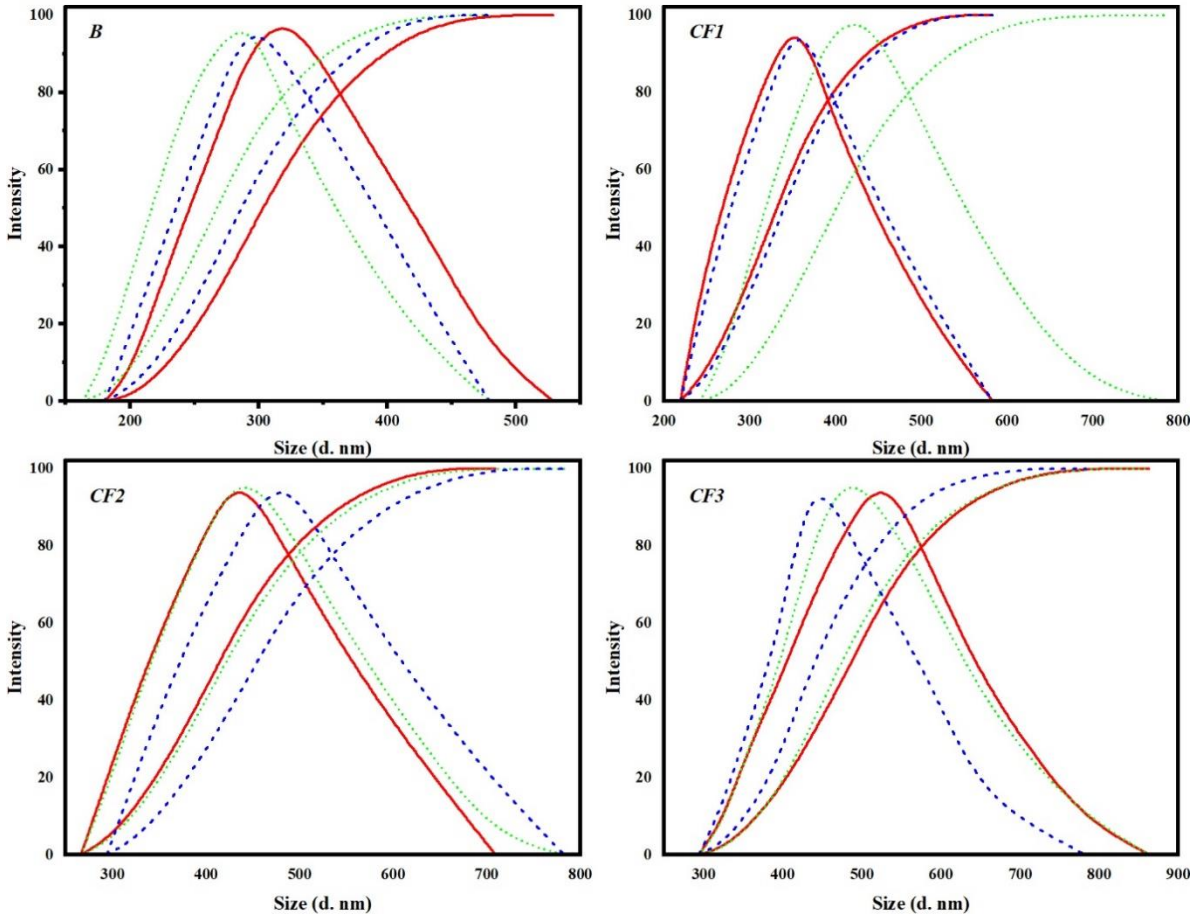

Fig. 4. DLS measured particle size distribution curves of different formulations (samples B, CF1, CF2 and CF3). Colors (red, blue and green) relate to the repeat of the samples

[DOI: 10.22068/ijmse.3913]

The resultant effect is a pronounced reduction in the contact angle, reflecting an improved spreading and adhesion profile on hydrophilic substrates, which is paramount for biomedical applications involving targeted drug delivery systems [28].
In this context, the hydrophilic nature of folate, integrated within the castor folate ester, plays a pivotal role in modulating the wetting behavior of niosome formulations. Figure 5 shows images of the samples on the substrate, and the data is collected in Table 3. Table 3 presents the contact angles (θ) of the niosome formulations in comparison to the baseline formulation (doxorubicin hydrochloride solution in PBS), and the data is taken from figure 5. The empirical θ values, ranging from 64.6 ± 1.2° to 59.1 ± 2.9° for the niosomes and 52.9 ± 2.3° for the doxorubicin hydrochloride solution in PBS, underscore a significant enhancement in the wetting efficiency of the niosomes ($P< 0.05$). This phenomenon is indicative of a robust interaction between the hydrophilic folic acid moieties and the solid substrate, which facilitates a more energetically favorable conformation compared to the aqueous doxorubicin solution and indicates doxorubicin hydrochloride, as a hydrophilic molecule, is expected to have a higher loading efficiency in samples containing higher amounts of folate molecules.

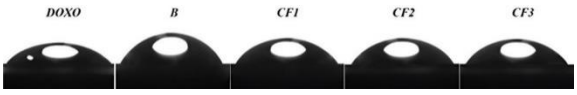

Fig. 5. Images of the samples on the substrate

Table 3. Water contact angle for different niosomes formulations

Sample Code	Water Contact Angle, θ (°)
DOX Solution	52.9 ± 2.3
B	64.6 ± 1.2
CF1	63.3 ± 1.8
CF2	61.7 ± 1.6
CF3	59.1 ± 2.9

3.2.4. Release profile

Figure 5 details the encapsulation efficiency of DOX within the formulated niosomes. It is observed that niosomes with a higher concentration of castor-folate exhibit increased loading of DOX. The higher hydrophilic nature of CF can explain this phenomenon, which is modified noisome relative to pure noisome, as confirmed by water contact angle results that facilitate greater incorporation of the hydrophilic drug in noisome vesicles.
This trend aligns with the observed increment in particle size; larger niosomes possess a higher surface area, potentially increasing the loading capacity. Folic acid's hydrophilic groups in castor-folate contribute to this effect by promoting lipid-drug interactions.
The mechanism of drug release from vesicular systems is usually based on concentration differences or disruption of the vesicle membrane structure [29]. These laboratory results show that the release of doxorubicin is much slower than the free drug, and in sample CF1, only about 40% of the drug was released after 24 hours, which indicates a delayed release of the synthesized niosomal system.
Figure 7. depicts the release profile of doxorubicin hydrochloride from different noisome formulations. Over time, there is a progressive increase in the amount of drug released. The release rate is initially rapid within the first 10 hours, followed by a deceleration. Niosomes with a higher percentage of castor-folate demonstrate a more substantial drug release. This behavior is attributable to the hydrophilic nature of the folate molecule within the castor-folate, which enhances the solubility of doxorubicin hydrochloride in the lipid wall, thus facilitating its migration out of the niosome. Interestingly, despite the larger particle size of these niosomes, which typically suggests a lower release level, the release rate of doxorubicin hydrochloride is higher. This indicates that the improved solubility of the drug in the lipid wall plays a dominant role due to the increased presence of castor-folate. Additionally, it is essential to consider that niosomes with a higher castor-folate content have a greater initial drug loading, which may contribute to the observed release patterns.

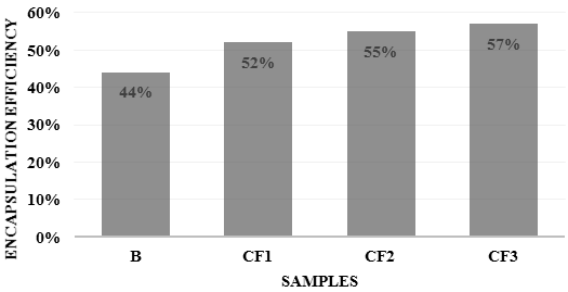

Fig. 6. The loading amount of DOX drug in different formulations

[DOI: 10.22068/ijmse.3913]

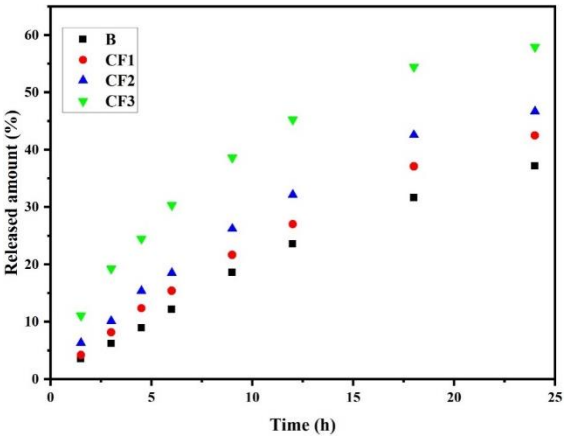

Fig. 7. DOX drug released at different times

3.2.5. Biotoxicity of niosomes

The empirical data, meticulously tabulated in Table 4, unequivocally demonstrates that the fibroblast cells maintained a high level of metabolic activity (79% cell viability) when exposed to the niosomes containing doxorubicin and without surface modification by castor folate (sample B). This vital observation was quantified by comparing the viability indices to the baseline established by the negative control, which was set at an absorbance indicative of 100% cell viability. The robust cellular activity observed suggests that the niosomes provide a conducive environment for cell growth and function, a critical parameter in assessing biomaterials for clinical applications [30].

In niosomes modified with castor folate, we observed decreased cell viability. As shown in Table 4, the approximate toxicity of the formulations containing 5%, 10%, and 15% castor folate is 66%, 61%, and 59%, respectively. This indicates that folate increases the toxicity of the drug on fibroblast cells. This is probably due to the involvement of the folate molecule in the mechanism of binding of niosomal carriers to the cell surface [31].

The synthesized niosomes with castor-folate stand out as a noteworthy advancement in drug delivery. Their proven biocompatibility paves the way for subsequent research and development efforts to harness their unique properties for targeted therapeutic applications. The potential for these niosomes to revolutionize the delivery of medical treatments is immense, offering a glimpse into a future where the efficacy and precision of drug administration are significantly enhanced.

Table 4. Cytotoxicity test results by direct method

Sample Code	Cell Viability (%)
B	79.31
CF1	65.91
CF2	60.92
CF3	59.29

4. CONCLUSIONS

In conclusion, the present study has elucidated the role of castor folate ester in the architectural integrity of niosomal lipid bilayers. The esterification of castor oil with folic acid has successfully encapsulated the chemotherapeutic agent doxorubicin hydrochloride. The morphological assessment via scanning electron microscopy affirmed the spherical configuration of the resultant niosomes.

Quantitative analysis revealed that the niosomal particle size is directly proportional to the castor folate content, likely due to the lipid matrix's elevated hydrophilic-lipophilic balance (HLB). The zeta potential measurements indicated a pronounced stability of the niosomes, attributed to the substantial negative surface charge. Increased castor folate concentration also resulted in a higher contact angle and drug loading efficiency, suggesting enhanced hydrophilicity and particle size.

The drug release kinetics of the niosomes exhibited a controlled and sustained profile, with an observed increase in the release rate concomitant with higher folate castor levels. Cytocompatibility studies, including the MTT assay and interactions with L929 fibroblast cells, demonstrated the biocompatible nature of the niosomes, validating their potential as a non-toxic vehicle for doxorubicin hydrochloride delivery.

The findings of this research advocate for the incorporation of folate castor ester as an efficacious additive in niosomal formulations, optimizing both the physicochemical properties of the lipid bilayer and the overall drug delivery efficacy.

CREDIT AUTHORSHIP CONTRIBUTION STATEMENT

Amin Rahiminejad: Investigation, Resources, Writing- Original draft preparation, Visualization. **Mojgan Heydari:** Conceptualization, Methodology, Validation, Formal analysis, Writing- Reviewing and Editing, Supervision, Project administration,

[DOI: 10.22068/ijmse.3913]

Funding acquisition.
Fariba Tajabadi: Conceptualization, Methodology, Validation, Formal analysis, Writing- Reviewing and Editing, Supervision, Project administration.

DECLARATION OF COMPETING INTEREST

The authors declare that they have no known competing financial interests or personal relationships that could have appeared to influence the work reported in this paper.

DATA AVAILABILITY

Data will be made available on request.

ACKNOWLEDGMENTS

This project was financially supported by the Materials and Energy Research Center (MERC, Iran) with project number 781401051.

REFERENCES

[1]. Siepmann, J. and F. Siepmann. Microparticles Used as Drug Delivery Systems. in Smart Colloidal Materials. 2006. Berlin, Heidelberg: Springer Berlin Heidelberg.
[2]. Abd-Elghany, A.A. and E.A. Mohamad, Chitosan-coated niosomes loaded with ellagic acid present antiaging activity in a skin cell line. ACS omega, 2023. 8(19): p. 16620-16629.
[3]. S. Yasamineh, P. Yasamineh, H. Ghafouri Kalajahi, O. Gholizadeh, Z. Yekanipour, H. Afkhami, A state-of-the-art review on the recent advances of niosomes as a targeted drug delivery system. International journal of pharmaceutics, 2022. 624: p. 121878.
[4]. T. Piri-Gharaghie, N. Jegargoshe-Shirin, S. Saremi-Nouri, S.-h. Khademhosseini, E. Hoseinnezhad-lazarjani, A. Mousavi, Effects of Imipenem-containing Niosome nanoparticles against high prevalence methicillin-resistant Staphylococcus Epidermidis biofilm formed. Scientific reports, 2022. 12(1): p. 5140.
[5]. J. K. Patra, G. Das, L. F. Fraceto, E. V. R. Campos, M. d. P. Rodriguez-Torres, L. S. Acosta-Torres, Nano based drug delivery systems: recent developments and future prospects. Journal of nanobiotechnology, 2018. 16: p. 1-33.
[6]. B. Honarvari, S. Karimifard, N. Akhtari, M. Mehrarya, Z. S. Moghaddam, M. J. Ansari, Folate-targeted curcumin-loaded niosomes for site-specific delivery in breast cancer treatment: In silico and In vitro study. Molecules, 2022. 27(14): p. 4634.
[7]. Rishi Paliwal, Pramod Kumar, Shivani Rai Paliwal, Rameshroo Kenwat, Otmar Schmid, Utility of Nanomaterials in Nanomedicine for Disease Treatment, in Nanomaterials in Bionanotechnology. 2021, CRC Press. p. 333-359.
[8]. M. Moghtaderi, K. Sedaghatnia, M. Bourbour, M. Fatemizadeh, Z. Salehi Moghaddam, F. Hejabi, Niosomes: a novel targeted drug delivery system for cancer. Medical Oncology, 2022. 39(12): p. 240.
[9]. Zhoujiang Chen, R.K.K., Lianlin Long, Songzhi Xie, AiZheng Chen, Liang Zou, Current understanding of passive and active targeting nanomedicines to enhance tumor accumulation. Coordination Chemistry Reviews, 2023. 481.
[10]. Wang, F., Development and characterization of folic acid-conjugated chitosan nanoparticles for targeted and controlled delivery of gemcitabinein lung cancer therapeutics. Artificial cells, nanomedicine, and biotechnology, 2017. 45(8): p. 9.
[11]. B. Bahrami, M. Mohammadnia-Afrouzi, P. Bakhshaei, Y. Yazdani, G. Ghalamfarsa, M. Yousefi, Folate-conjugated nanoparticles as a potent therapeutic approach in targeted cancer therapy. Tumor Biology, 2015. 36(8): p. 5727-5742.
[12]. M. Safari Sharafshadeh, F. Tafvizi, P. Khodarahmi and S. Ehtesham, Folic acid-functionalized PEGylated niosomes co-encapsulated cisplatin and doxoribicin exhibit enhanced anticancer efficacy. Cancer Nanotechnology, 2024. 15(1): p. 14.
[13]. Kawano, K. and Y. Maitani, Effects of polyethylene glycol spacer length and ligand density on folate receptor targeting of liposomal Doxorubicin in vitro. J Drug Deliv, 2011. 2011: p. 160967.
[14]. K. Knop, R. Hoogenboom, D. Fischer and U. S. Schubert, Poly(ethylene glycol) in Drug Delivery: Pros and Cons as Well

[DOI: 10.22068/ijmse.3913]

as Potential Alternatives. Angewandte Chemie International Edition, 2010. 49(36): p. 6288-6308.
[15]. G. Liu, Y. Li, L. Yang, Y. Wei, X. Wang, Z. Wang, Cytotoxicity study of polyethylene glycol derivatives. RSC Advances, 2017. 7(30): p. 18252-18259.
[16]. Rajalakshmi, P., J.M. Marie, and A.J. Maria Xavier, Castor oil-derived monomer ricinoleic acid based biodegradable unsaturated polyesters. Polymer Degradation and Stability, 2019. 170: p. 109016.
[17]. Saeedi, S., S. Murjan, and M.R. Nabid, Redox and pH dual sensitive folate-modified star-like amphiphilic copolymer based on castor oil for controlled doxorubicin delivery. Journal of Drug Delivery Science and Technology, 2021. 62: p. 102391.
[18]. M. Wang, J. Long, S. Zhang, F. Liu, X. Zhang, X. Zhang, Folate-Targeted Anticancer Drug Delivery via a Combination Strategy of a Micelle Complex and Reducible Conjugation. ACS Biomaterials Science & Engineering, 2020. 6(3): p. 1565-1572.
[19]. M. Jurczyk, K. Jelonek, M. Musiał-Kulik, A. Beberok, D. Wrześniok and J. Kasperczyk, Single- versus Dual-Targeted Nanoparticles with Folic Acid and Biotin for Anticancer Drug Delivery. Pharmaceutics, 2021. 13(3): p. 326.
[20]. Y. Ge, M.-H. Kwon, F. Kou, R. A. Uthamapriya, P. Zhang, D.-J. Lee, Folic-acid-targeted drug delivery system implementing Angelica gigas polysaccharide: A potential strategy for colorectal cancer treatment. International Journal of Biological Macromolecules, 2024. 283: p. 137653.
[21]. Yoshioka, T., B. Sternberg, and A.T. Florence, Preparation and properties of vesicles (niosomes) of sorbitan monoesters (Span 20, 40, 60 and 80) and a sorbitan triester (Span 85). International Journal of Pharmaceutics, 1994. 105(1): p. 1-6.
[22]. E. Gianasi, F. Cociancich, I. F. Uchegbu, A. T. Florence and R. Duncan, Pharmaceutical and biological characterisation of a doxorubicin-polymer conjugate (PK1) entrapped in sorbitan monostearate Span 60 niosomes. International Journal of Pharmaceutics, 1997. 148(2): p. 139-148.
[23]. Florence, A.T. and D. Attwood, Properties of the Solid State, in Physicochemical Principles of Pharmacy, A.T. Florence and D. Attwood, Editors. 1998, Macmillan Education UK: London. p. 5-35.
[24]. Standard, I., Biological evaluation of medical devices—Part 5: Tests for in vitro cytotoxicity. Geneve, Switzerland: International Organization for Standardization, 2009. 10: p. 9781570203558.
[25]. M. Razaghpour, R. Mohammad Ali Malek, M. Montazer and S. Ramezanpour, Cellulose cross-linking with folic acid at room via diverse-based coupling reagents attaining multifunctional features. Carbohydrate Polymers, 2023. 302: p. 120376.
[26]. T. Panhwar, S. Mahesar, A. Kandhro, S. Sheerazi, A. Kori, D. Laghari, Physicochemical composition and FTIR characterization of castor seed oil. Ukrainian Food Journal, 2019. 8: p. 778-787.
[27]. F. N. Parın, S. Ullah, K. Yildirim, M. Hashmi and I.-S. Kim, Fabrication and Characterization of Electrospun Folic Acid/Hybrid Fibers: In Vitro Controlled Release Study and Cytocompatibility Assays. Polymers, 2021.
[28]. H. Abdelkader, Z. Wu, R. Al-Kassas and R. G. Alany, Niosomes and discomes for ocular delivery of naltrexone hydrochloride: Morphological, rheological, spreading properties and photo-protective effects. International Journal of Pharmaceutics, 2012. 433(1): p. 142-148.
[29]. Hughes, G.A., Nanostructure-mediated drug delivery. Nanomedicine, 2005. 1(1): p. 22-30.
[30]. M. Barani, M. Mirzaei, M. Torkzadeh-Mahani, A. Lohrasbi-Nejad and M. H. Nematollahi, A new formulation of hydrophobin-coated niosome as a drug carrier to cancer cells. Materials Science and Engineering: C, 2020. 113: p. 110975.
[31]. C. He, M. Heidari Majd, F. Shiri and S. Shahraki, Palladium and platinum complexes of folic acid as new drug delivery systems for treatment of breast cancer cells. Journal of Molecular Structure, 2021. 1229: p. 129806.

[DOI: 10.22068/ijmse.3913]